Paper presented at the IEEE 1996 Nuclear Science
Symposium & Medical Imaging Conference
Anaheim, California
November 2-9, 1996

HH-96-4

Correlation of Radiation Damage Effects in High Resistivity Silicon Detectors with Results from Deep Level Spectroscopy*

**H. Feick, E. Fretwurst,
G. Lindström, and M. Moll**

I. Institut für Experimentalphysik, Universität Hamburg, Germany

to be published in the conference issue of the
IEEE Transactions on Nuclear Science

*This research was supported by the BMFT
Contract No. 05 7HH 17I

Correlation of Radiation Damage Effects in High Resistivity Silicon Detectors with Results from Deep Level Spectroscopy[1]

H. Feick, E. Fretwurst, M. Moll, and G. Lindström

I. Institut für Experimentalphysik, Universität Hamburg, Luruper Chausse 149, 22761 Hamburg, Germany

Abstract

Neutron irradiated high resistivity silicon detectors have been subjected to isochronous annealing in order to study the changes in the full depletion voltage and the leakage current. The corresponding evolution of bulk damage induced defect levels was monitored using the TSC method. A single TSC peak is found to be correlated with the transient decay of the depletion voltage which is observed after elevated temperature annealing of inverted detectors. In conjunction with deep level parameters obtained from an I-DLTS study and changes observed in the effective doping concentration and in the leakage current after exposure to high doses of ^{60}Co-gammas, new insight is gained into the radiation induced device deterioration and the corresponding annealing behavior.

I. INTRODUCTION

Silicon detectors fabricated from high resistivity float-zone silicon are frequently applied in high energy physics experiments for particle tracking and vertexing purposes. The basic structure is a p^+-n-n^+ reach-through diode with thin (< 0.1 μm) ion-implanted junction (p^+) and ohmic contact (n^+) on the front and rear side of a thick (around 300 μm) high resistivity bulk material. They are known to exhibit a change in the reverse bias voltage required for full activation (V_{dep}) and an increase in the leakage current (I) when operated in an environment with high radiation levels (π, n, p, etc.) which is now agreed on to impose the operation life-time limit of such devices [1]. The deterioration is explained in terms of radiation induced bulk defects which form electrically active levels in the forbidden gap of the semiconductor. The full depletion voltage is related to the effective doping concentration N_{eff} by

$$V_{dep} \approx \frac{q_0}{2\varepsilon\varepsilon_0} d^2 |N_{eff}|, \qquad (1)$$

where q_0 means the elementary charge, $\varepsilon\varepsilon_0$ is the permittivity of silicon, and d is the thickness of the device. The built-in voltage of the junction has been neglected in the above expression since it is much smaller than practical values of the reverse biases. It must be born in mind that N_{eff} depends on the ionization state of the defect levels in the material (shallow doping, e.g. phosphorus *and* radiation induced levels) according to

$$N_{eff} = \sum_{donors} p_t - \sum_{acceptors} n_t \ , \qquad (2)$$

that is, by definition only donors occupied with holes (devoid of electrons) and acceptors occupied with electrons contribute to N_{eff}. For every trap the totality condition is fulfilled: $n_t + p_t = N_t$. In the thermal equilibrium state, e.g. in the not depleted neutral bulk of the diode, the ionization state is given by the position of the Fermi-level E_F relative to the energetic position of the levels, whereas in the depleted zone steady state values n_t* and p_t* are maintained by the successive emission of electrons and holes into the conduction and valence band at the rates e_n and e_p, respectively,

$$n_t^* = \frac{N_t}{1+e_n/e_p}, \ p_t^* = \frac{N_t}{1+e_p/e_n}. \qquad (3a,b)$$

This result follows from standard Shockley-Read-Hall statistics when the capture of free carriers, that may exist in the depleted zone due to leakage currents, is neglected [2]. More general treatments have recently been discussed in the references [3] and [4]. The emission rates strongly depend on the trap energy E_t and the absolute temperature T,

$$e_{n,p} = c_{n,p} n_i \exp\left(\pm \frac{E_t - E_i}{k_B T}\right). \qquad (4)$$

Here $c_{n,p}$ denotes the capture coefficient for electrons or holes, n_i and E_i mean the carrier concentration and the position of the Fermi-level in the intrinsic semiconductor, which is close to the middle of the gap (see [5]), and k_B is the Boltzmann-constant. It is noted that E_t is a Gibbs-free energy in the thermodynamical sense, compare [6]. A complete characterization of a trap is established experimentally by determining the temperature dependent capture rates for both, electrons and holes, i.e., $c_n(T)$ and $c_p(T)$, and a pair ($\Delta H_{n,p}$, $X_{n,p}$) of ionization enthalpy and entropy factor either related to the conduction band E_C (electron traps) or related to the valence band E_V (hole traps). The corresponding Gibbs-free energy position is then given by

$$\begin{aligned} E_C - E_t &= \Delta H_n - k_B T \ln(X_n) \quad \text{e - traps} \\ E_t - E_V &= \Delta H_p - k_B T \ln(X_p) \quad \text{h - traps} \end{aligned} \qquad (5a,b)$$

where $(E_C - E_t) + (E_t - E_V) = E_g$ gives the temperature dependent energy gap. Despite these guide-lines a straight forward characterization is often done without measurement of the capture coefficients. These are then visualized to be the product of the carrier thermal velocity and a capture cross section $\sigma_{n,p}$ that is assumed to be temperature independent. Also in this work all level parameters were derived from Arrhenius-plots using the relation

$$e_{n,p} = B\left(\frac{m^*_{n,p}}{m_0}\right)\sigma_{n,p} T^2 \exp\left(-\frac{\Delta H_{n,p}}{k_B T}\right). \qquad (6)$$

[1]Work supported by the BMFT under contract 05 7HH 17I.

B is a constant equal to 3.256×10^{21} $K^{-2}cm^{-2}s^{-1}$ and $m^*_{n,p}/m_0$ denotes the density-of-states masses relative to the electron rest mass in the conduction (1.08) and valence band (0.549), respectively [5].

From the consideration of eqs. 2, 3, and 4 it can be concluded that only those acceptors located in the lower half and only those donors in the upper half of the band gap contribute to the space charge in the depletion region, provided the capture coefficients c_n and c_p are of the same order of magnitude. It is known that the changes in the full depletion voltage as function of the irradiation fluence Φ roughly can be regarded as to arise from the introduction of negative space charges at a rate around 0.1 cm^{-1} which eventually (e.g. $\Phi > 10^{13}$ cm^{-2} for the material used here) inverts the sign of N_{eff} in the depleted zone from initial plus to minus (so-called inverted detectors). On the other hand, the introduction rates of the dominant defect levels (VO_i, C_iO_i, $V\,V$, C_iC_s), which all would not affect N_{eff} according to the above stated, have been found to be of the order of 1 cm^{-1} [7]. Therefore, special care was taken of defects exhibiting small introduction rates since they may have been overlooked in previous works.

The leakage current I which is generated per depleted volume V by a particular level of concentration N_t is written (see for example [8])

$$I\,/V = q_0 \frac{e_n e_p}{e_n + e_p} N_t \,. \qquad (7)$$

Normalizing this relation with respect to the fluence Φ then gives the leakage current related damage constant $\alpha = I/(V\Phi)$ as function of the defect introduction rate $g_t = N_t/\Phi$. It is evident from eq. (7) that, given the capture coefficients c_n and c_p are of the same order, traps with a Gibbs-free energy E_t close to the intrinsic Fermi-level E_i will be most efficient. Moreover, regarding eq. 3, also a significant ionization would be expected. Accordingly, special interest must be paid to such levels.

The bulk of this paper deals with an isochronous annealing study which correlates the behavior of the full depletion voltage and the leakage current with spectroscopic information obtained from Thermally Stimulated Current (TSC) measurements. Additional information concerning the deep level parameters is obtained from Current-Deep Level Transient Spectroscopy (I-DLTS) studies. Moreover the changes in the N_{eff} and leakage current observed after exposure to very high doses of ^{60}Co-gammas will be presented. These are of special interest because the generated bulk defects are randomly distributed. In contrast to this, high energetic heavy particles give rise to regions of increased defect density and in addition introduce a larger fraction of higher order multi-vacancy defects, e.g. divacancies.

Previous correlation studies of this kind can be found in the references [2,9,10]. While most of those papers have mainly considered the leakage current, we will also present significant new results regarding the effective doping concentration.

II. Isochronous Annealing Study

A. Experimental Procedure

Two p^+-n-n^+ silicon diodes fabricated by the Max-Planck Institute (MPI) München from 3kΩcm float-zone silicon were used. The devices are d = 280 µm thick and it has been inferred from proton micro-beam measurements that the active area, A, is given by 0.275 cm^2 [11,12]. This value is larger than the size of the implanted pad electrode (0.5×0.5 cm^2) because of the lateral extension of the depleted zone. Irradiations with fast neutrons ($\langle E \rangle$ = 5.3 MeV) were performed at the Physikalisch-Technische Bundesanstalt (PTB) Braunschweig, Germany. For the calculation of equivalent 1-MeV-neutron fluences Φ the hardness factor 1.45 has been used, which is appropriate for this specific source [13]. One of the devices was irradiated beyond the fluence required to invert the sign of the space charge. Moreover, there was a considerable storage period of 420 d at room temperature prior to the experiment, for details see Table 1.

Table 1

Devices used for the annealing experiment. $N_{eff,0}$ and $N_{eff,i}$ denote the effective doping concentration prior to the irradiation and the first elevated temperature annealing, respectively.

	M20609	M20708
Φ	9.76×10^{11} cm^{-2}	3.82×10^{13} cm^{-2}
$N_{eff,0}$	1.39×10^{12} cm^{-3}	1.26×10^{12} cm^{-3}
$N_{eff,i}$	1.20×10^{12} cm^{-3}	-1.46×10^{12} cm^{-3}

The isochronous annealing procedure started at 50°C and 20°C temperature increments were chosen. After keeping the samples for around 90 min at the elevated temperature in normal atmosphere they were rapidly cooled down to room temperature for the measurements. TSC measurements were essentially performed as outlined in a previous paper [14]. A constant heating rate β = 0.183 K/s has always been used which allows a straight forward identification of most traps by the temperature at which the corresponding peaks occur. Moreover, the filling time was always equal to 30 s and the samples were warmed up to 290 K after every measurement to ensure reproducible conditions. Leakage currents have been subtracted from all spectra in this paper, the corresponding data were obtained from TSC runs in which intentionally no defects were filled.

B. Changes in V_{dep} and Leakage Current

Figure 1 displays the CV and IV data in the unannealed state and at the indicated stage of the isochronous annealing experiment. Apparently a breakdown occurs around 100 V for the not-inverted detector and around 200 V for the other sample. Since the full depletion voltage was increasing very much in the latter case, reasonable values of the leakage current at full depletion, I, could only be derived up to the

annealing step at 130°C whereas the depletion voltages, V_{dep}, could be determined by an extrapolation method up to the 210°C.

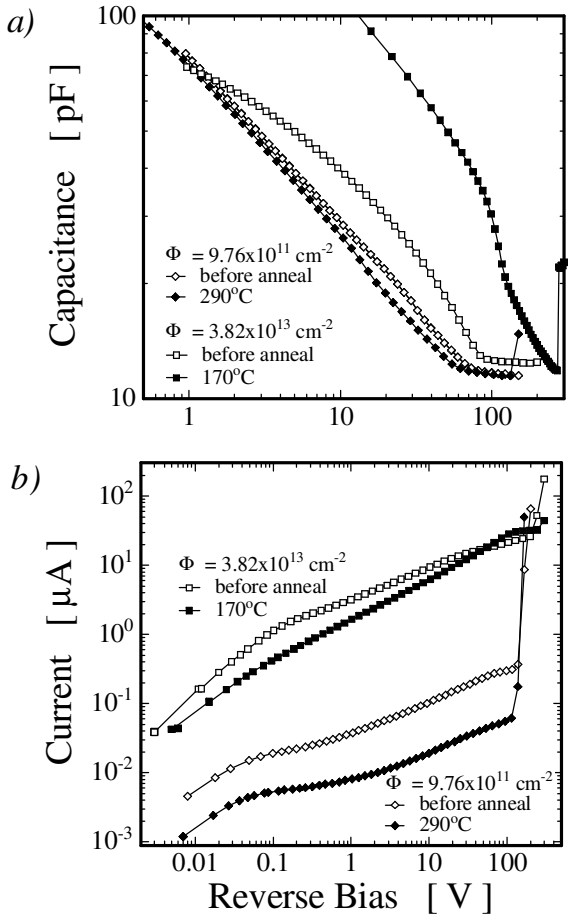

Figure 1: CV a) and IV b) curves before the first annealing step and at a later stage of the isochronous annealing study.

Effective doping concentrations were calculated from V_{dep} according to eq. (1) and leakage currents have been corrected to equivalent 20°C values. After normalization to the appropriate fluence the data were plotted as function of the isochronous annealing temperature in Figure 2. It will be noted that the deviation $\Delta N_{eff}(T) := N_{eff,i} - N_{eff}(T)$ with respect to the value before elevated temperature annealing, $N_{eff,i}$, is given. ΔN_{eff}, which is an increasingly positive number when negative space charge is introduced by the annealing, exhibits the so-called reverse annealing effect. This is composed of several stages, as was already noted in [15]. The first stage, which is of prime importance for the long term operation of silicon detectors, is indicated at the data measured on the heavily damaged sample. No corresponding annealing stage can be identified for the weakly damaged sample, rather do the data presented in Figure 2a) provide evidence for markedly different annealing kinetics to prevail in the low fluence range. Furthermore, from the IV data obtained on the weakly damaged device it can be inferred that the bulk generation current shows beneficial annealing only. In inverted devices, where the junction has switched to the back plane contact and therefore is not supplied with an edge protection anymore, the reduction is screened by excessive edge leakage currents occurring at higher bias voltages. Thus, only the data measured on the weakly damaged device is believed to reasonably well represent the annealing of the bulk leakage current generation centers (Figure 2b).

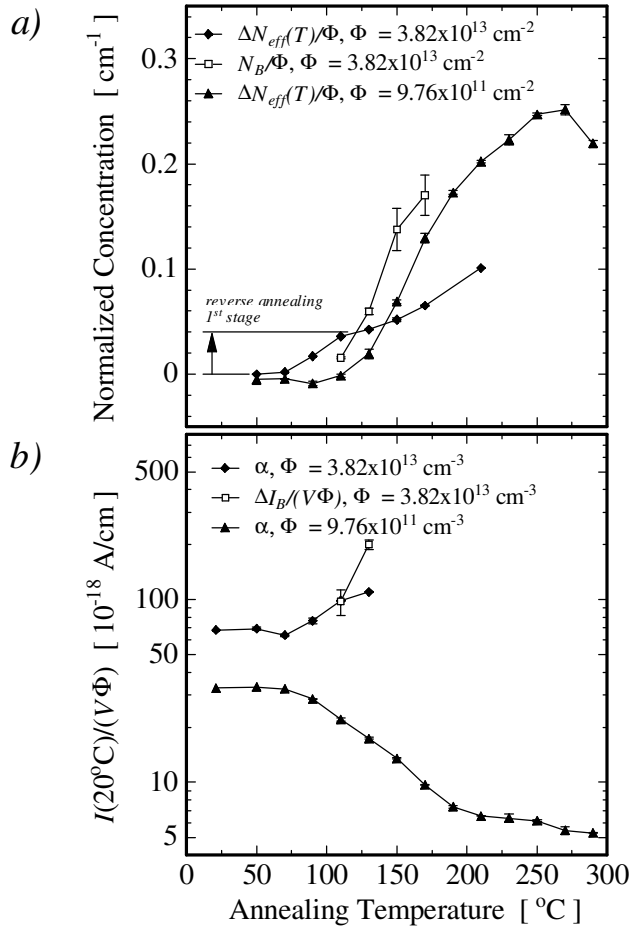

Figure 2: Fluence normalized values of the effective doping concentration a) and the leakage current at full depletion per volume b) as function of the annealing temperature (N_B and ΔI_B see text).

Besides the overall variations of the effective doping concentration and the bulk leakage current, which can be exploited for the correlation with microscopic defect studies, there is also a transient effect arising from the elevated temperature annealing in inverted detectors manifested by a decay of the depletion voltage from an excited value, observed right after quenching the sample to room temperature, towards a steady-state value. Corresponding observations were made on the sample M20708, see Figure 3. This subject has previously been studied in detail by our group in reference [16] and was discussed there in terms of a bistable defect reaction. Prolonged annealing at temperatures greater than 80°C thereafter introduces a bistable complex defect with the two states A and B. The latter is activated by thermal agitation, forward current injection, or illumination and decays via a simple dissociation process into state A which therefore may be visualized to consist of two components, A1 and A2. The amplitude, the time constant, and the steady

state value of the depletion voltage transient seen in Figure 3 was determined by fitting an exponential decay model to the data with the time scale taken as zero at the end of the preceding annealing procedure. For annealing temperatures ranging from 110°C to 170°C the concentration of introduced bistable defects in the state B, N_B, was calculated from the amplitude using eq. (1), see Figure 2a).

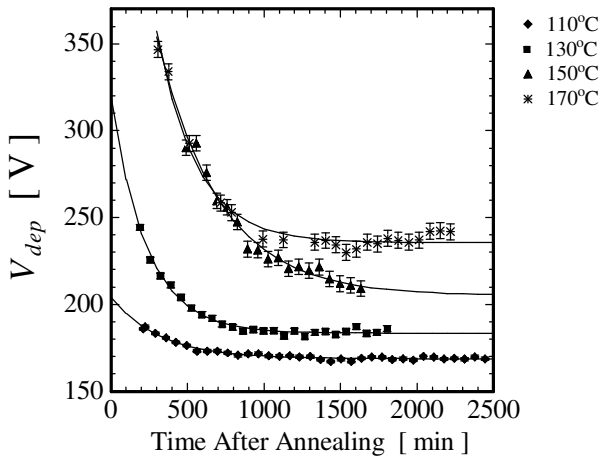

Figure 3: Transient effect observed on the depletion voltage after quenching the sample M20708 from the indicated annealing temperature to room temperature (solid lines: fit).

Also the IV data exhibit a transient decay, it is however not clear whether the leakage current reflects a mid-gap generation center related to state B of the bistable defect or is due to an increase of the edge currents and thus merely correlated to the V_{dep} decay. The amplitude ΔI_B of the declining current has been determined using the same fitting procedure as for the depletion voltage (Figure 2b).

C. Microscopic Observations

After having explored all macroscopic effects encountered during the isochronous annealing of the two samples, it will now be discussed in detail which coincident processes could be detected on the microscopic scale using the TSC method. It must be born in mind that, as discussed in reference [14], the filling conditions strongly influence the obtained spectra. In order to gain a comprehensive representation of all defect levels, various sets of measurement parameters have been applied. Table 2 gives the peak labels and the according temperatures at which the emission current was found to be maximized in the figures that follow. In addition the type of the defect, which can be inferred when different filling modes are taken into consideration, and the most likely assignment to a chemical defect is given for better orientation, compare also [14].

First, the results obtained on the weakly damaged device ($\Phi \approx 10^{12}$ cm^{-2}) will be presented. To avoid current injection from the back plane contact during the TSC measurement, the reverse bias has been fixed to 50 V closely below the full depletion voltage. Figure 4a) displays the variation of the TSC spectrum in which electron traps were filled by cooling down under zero bias. In this filling mode the occupation of the electron traps is determined by the Fermi-level, E_F, which is close to the middle of the band gap at room temperature and sweeps across the deep levels in the upper half of the band gap towards the conduction band with decreasing temperature. One shortcoming of this method is that E_F may pin at a specific level when all free electrons from the conduction band are trapped into deep levels (compensation). In the early stages of the annealing experiment peak *N* always compensates for all of the positive space charges, thus no deep traps but those causing the TSC signal *N* were filled. After the 150°C anneal, the left-hand side of the composed peak *N* started to anneal out and, following the 210°C anneal, the remaining fraction, N_c, could successfully be characterized using the delayed heating method, see Table 2. Finally, at the 290°C anneal, an electron trap emerges, causing a TSC peak at around 145 K, labeled *L'*. The annealing of peak *N* reduces the compensation and therefore enables the partial filling of traps further away from the middle of the band gap. Depending on the concentrations of the deeper levels (*L'* and *N*), the heights of the peaks *F* and *I* are modified accordingly, which must not be confused with a real annealing effect.

Table 2

Compilation of the peaks found in the TSC spectra (heating rate $\beta = 0.183$ K/s). The level parameters of the divacancy were derived from delayed heating measurements, see text.

	T_{max} [K]	Type	Assignment
A	34.2	*e*	?
B	39.6	?	?
C	48.0…47.1	*e*	$C_iC_s(B)^{(-/0)}$ …?
F	70.0	*e*	$VO_i^{(-/0)}$ (+$C_iC_s(A)^{(-/0)}$)
H	89.7	*h*	$VV^{(+/0)}$
I	95.6…99.1	*e*	$VV^{(--/-)}$ …?
J	116.2	*h*	? ($C_i^{(+/0)}$)
J'	120.6	*e*	?
Q	125.8	*h*	?
K	137.3	*h*	?
L'	146.3	*e*	?
M	147.2	*h*	$C_iO_i^{(+/0)}$
N	164.1	*e*	? + $VV^{(-/0)}$
N_c	167.2	*e*	$VV^{(-/0)}$ $\Delta H_t = 0.418$ eV $\sigma_n = 1.63\times10^{-15}$ cm^2
N_d	≈ 175	*h*	?

Figure 4b) shows the corresponding spectra where both, electron and hole traps have been filled by applying a forward injection current at low temperature. Several filling temperatures have been used and the curves presented in Figure 4b) were combined in such a way, that the optimum filling condition of the individual deep levels are represented, see caption. The filling of the hole traps *J* and *Q*, which are annealing in, is actually improved for 20 K injection, which

has however not been included in the figure. It is noted that under these experimental conditions peak *N* shifts further to higher temperatures than observed in Figure 4a). *A* hole trap, N_d, must therefore be concluded to grow on the right-hand side of *N* at the later annealing stages.

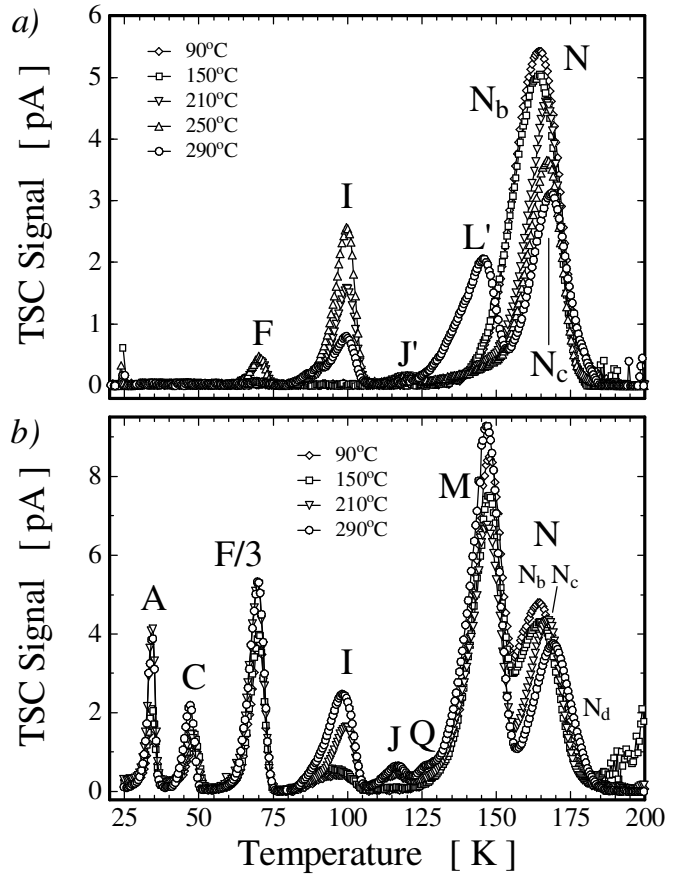

Figure 4: Isochronous annealing of the TSC spectrum measured on the device M20609 ($\Phi \approx 10^{12}$ cm^{-2}). a) After filling electron traps by cooling down under zero bias. b) Composite TSC spectra obtained after filling electron and hole traps by applying a 30 s long injection pulse of 1.7 mA at an appropriate temperature: 25 K for peaks A and C, 50 K for peak F, and 80 K for peaks I through N. Peak F, which is assumed to arise only from VO_i under these filling conditions, has been scaled down by a factor of 3 for better visibility.

Concentrations of defect levels, N_t, were derived from the TSC spectra by simply integrating the current emitted from a particular trap. The corresponding electric charge, Q_t, can be written

$$Q_t = \frac{1}{2} q_0 N_t A W \tag{8}$$

where W denotes the width of the depletion region. W can be calculated from the applied reverse bias voltage, V_{bias}, and the effective doping concentration, N_{eff}, in analogy to eq. (1)

$$W \approx \left(\frac{2\varepsilon\varepsilon_0}{q_0 |N_{eff}|} V_{bias} \right)^{1/2}. \tag{9}$$

Now, the concentration of filled deep levels affects the effective doping concentration, i.e., N_{eff} becomes a function of the TSC measurement temperature. Accordingly a first order correction has been applied to the evaluated data which is presented in Figure 5a) and b). It will be noted that the concentration of peak *N* given for the first annealing temperatures is too small due to the compensation effect. Moreover, the strong increase of peak *M* at the end of the experiment is probably due to the emergence of peak *L'*. Figure 5c) displays the shift of the maximum temperature as it was observed on three peaks.

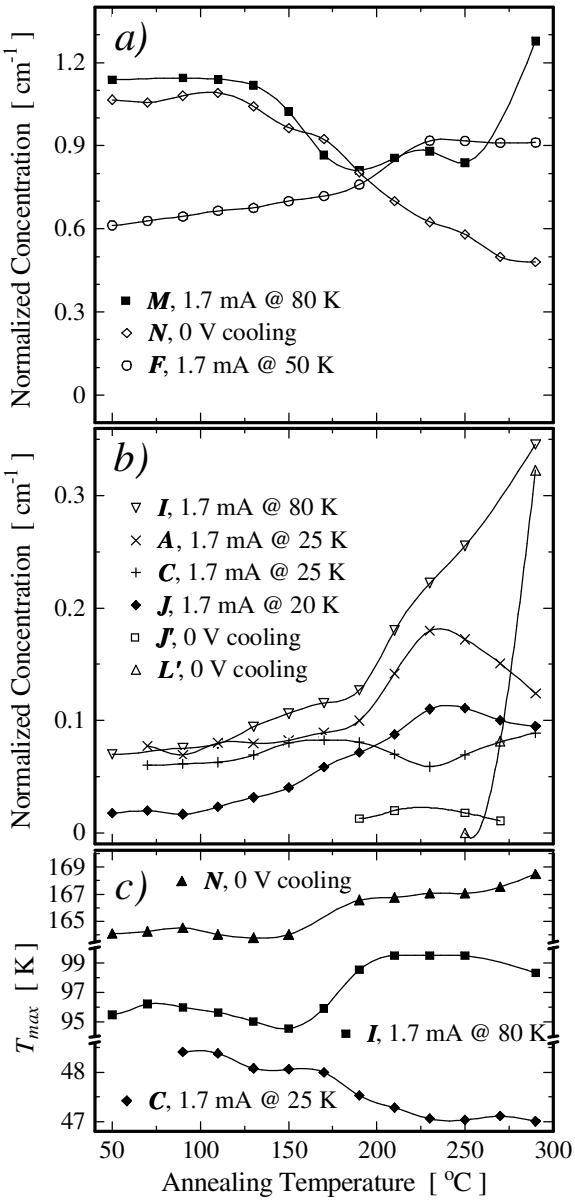

Figure 5: Evaluated peak concentrations normalized to the irradiation fluence a) dominant peaks b) smaller peaks, various filling methods were applied. c) Temperature shift of the peaks *N* , *I*, and *C* .

Figure 6a) shows the evolution of the TSC spectrum at three stages of the isochronous annealing as measured on the heavily damaged sample. A 1.7 mA forward current was injected for 30 s at 20 K which fills electron as well as hole

traps. The reverse bias voltage was 0.1 V because a small reverse bias was found to be suitable to overcome the deterioration of the spectra by the significant leakage current in inverted detectors. However, at the later stages of the annealing a useful spectrum is observed only for measurement temperatures below 150 K. It is not straight forward to derive concentrations from these TSC measurements because of the high defect concentrations [14], however, qualitatively the peaks *J*, *Q*, *H*, and *B* are found to grow in.

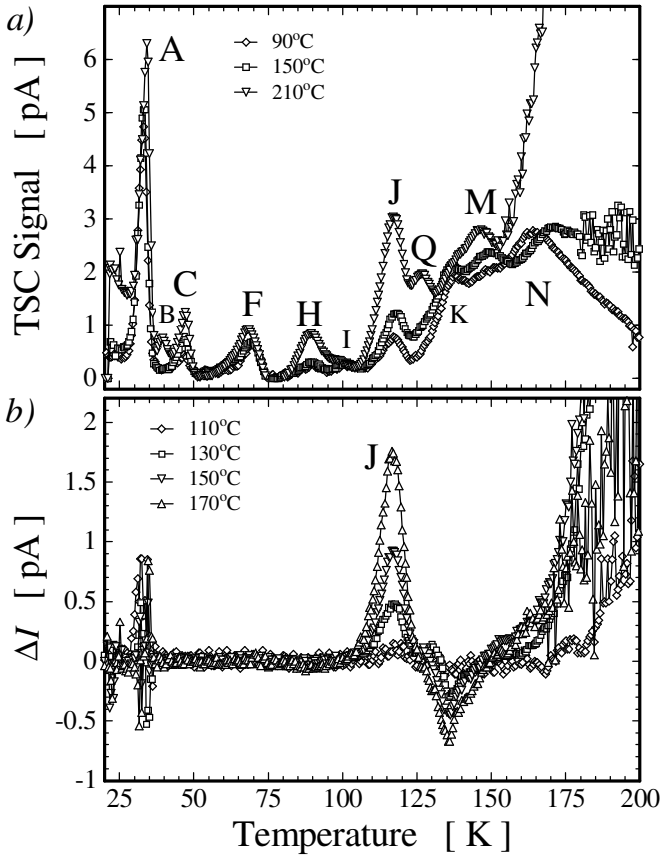

Figure 6: a) TSC spectra measured on the device M20708 ($\Phi \approx 4\times10^{13}$ cm^{-2}) after the indicated annealing step. b) Subtraction of the TSC spectrum measured before the excitation from the one measured afterwards. The modified depletion width after excitation in conjunction with the large leakage currents cause the increase of ΔI above 160 K.

The sample has been stored at room temperature for at least one day after quenching down from the annealing temperature to allow for the settling of the depletion voltage, compare Figure 3. After recording the TSC spectrum a forward current of 1.7 mA was injected for 20 min at 290 K which excites the bistable defect and results in a depletion voltage close to the value measured directly after the elevated temperature annealing [16]. On the thus prepared sample the TSC measurement was repeated. Figure 6b) shows the subtraction ΔI of the TSC spectrum before excitation from the one after excitation at four annealing temperatures. It is evident that only peak *J* does respond to the preparation of the excited state. This is the first time that we have observed such a close relationship between the change in a macroscopic property (V_{dep}) and a sole defect level (peak *J*).

III. I-DLTS Measurements

Deep levels have been characterized in high resistivity silicon detectors applying the I-DLTS technique. The samples were reverse biased for the measurements and the junction was illuminated with above band gap light for defect filling. At the time t_0 after the end of the filling pulse the decaying current signal was stored in a transient recorder using a period width T_W. To improve the signal to noise ratio the transients were averaged several times. The first Cosine and Sine Fourier-coefficients were calculated for several ranges (full period, half period, quarter period, etc.) of the transient data. Figure 7 shows the Sine coefficient, b_1, of the full period width T_W = 51.2 ms as function of temperature exhibiting the characteristic DLTS-peaks. While the 670 nm laser light is absorbed immediately below the junction and therefore only electrons drift through the field zone of the sample, the 980 nm light generates electron hole pairs homogeneously throughout the diode which fills electron (hole) traps only when $c_n > c_p$ ($c_n < c_p$). The inset in Figure 7 compares the low temperature part of the spectrum before and after irradiation. Here, 830 nm light, which penetrates significantly into the silicon, was used for the undamaged reference sample.

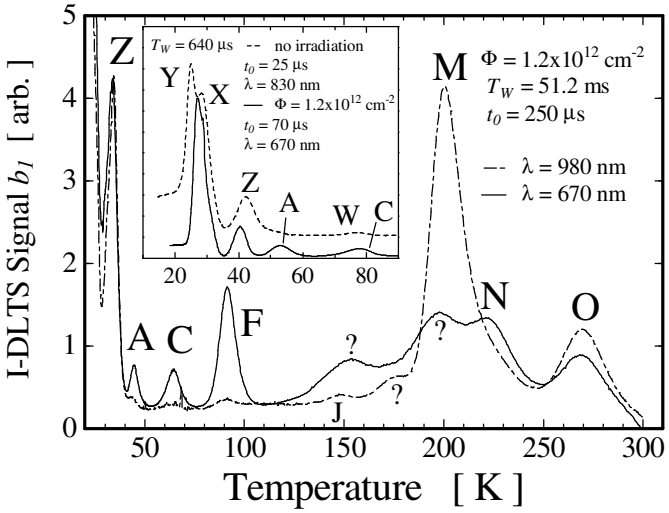

Figure 7: I-DLTS spectra measured on a Schottky diode (device 937K03) after neutron damage using two different wave lengths for the optical filling of the defects. The inset shows the low temperature part of the spectrum before (reference sample) and after irradiation.

Table 3 gives the results obtained from the Arrhenius plots. The temperatures at which the corresponding TSC peak would be expected has been used to assign the labels and the chemical nature for most of the observed levels, compare Table 2. Results from several measurements, as indicated in the second column of Table 3, have been averaged. Standard deviation errors are given to reflect the spread of the individual evaluations. Note, that the errors given for ΔH_t and σ are strongly correlated.

Table 3

Level parameters evaluated using the I-DLTS method.

	#		ΔH_t [meV]	σ_{lo}, σ_{ave}, σ_{hi} [cm^2]	Transition
X	5	*e*	42.6±4.4	(1.8, 5.7, 30)×10^{-14}	$P_s^{(0/+)}$?
Z	6	*e*	63.3±2.3	(2.7, 5.6, 12)×10^{-14}	TD ?
W	1	*e*	159	(-, 1.2, -)×10^{-11}	TD ?
A	7	*e*	78.5±3.8	(0.38, 1.0, 2.9)×10^{-14}	?
C	7	*e*	113±6.6	(2.1, 5.9, 17)×10^{-15}	$C_iC_s(B)^{(-/0)}$
F	6	*e*	169±3.2	(3.6, 6.1, 9.9)×10^{-15}	$VO_i^{(-/0)} + C_iC_s(A)^{(-/0)}$
J	3	*h*	315±18	(0.35, 1.7, 8.0)×10^{-13}	?
M	3	*h*	369±25	(0.65, 2.9, 13)×10^{-15}	$C_iO_i^{(+/0)}$
N	2	*e*	411±11	(0.99, 1.6, 2.6)×10^{-15}	? + $VV^{(-/0)}$
O	4	*e*	533±11	(2.3, 3.9, 6.7)×10^{-15}	?

IV. CO GAMMA IRRADIATIONS

A set of silicon detectors has been exposed to ^{60}Co-gamma radiation up to 500 Mrad at the Brookhaven National Laboratory (BNL). IV and CV curves have been measured for several months after the irradiation, however, no systematic annealing effect was observed in the full depletion voltage or the leakage current at full depletion. The latter is plotted in Figure 8a) after normalization to the detector volume and exhibits, within experimental errors, an increase proportional to the irradiation dose *D*. As for heavy particle irradiations the effective doping concentration is found to become more negative, and also the sign of the space charge is observed to become negative, as could be proven using TCT measurements, see [17]. Figure 8b) gives the change in the effective doping concentration $\Delta N_{eff} := N_{eff,0} - N_{eff}$ where $N_{eff,0}$ and N_{eff} denote the initial and the post irradiation value, respectively.

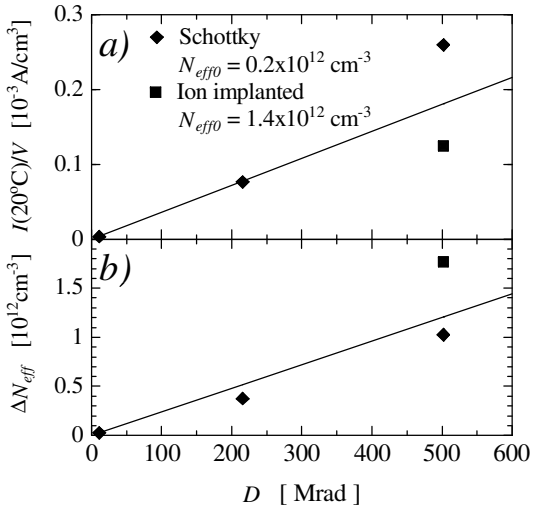

Figure 8: Leakage current increase a) and change in the effective doping concentration b) observed after ^{60}Co-gamma irradiation.

Since both quantities appear to increase proportional to the dose, the data have been normalized with respect to *D* and averaged afterwards, resulting in the data presented in Table 4. It should be noted that also the oxide surface of the devices becomes heavily damaged by the gamma rays and the leakage currents therefore are composed of bulk and surface generation currents. Only the ion implanted device was supplied with a guard-ring, which however was left floating. Proper contacting of the guard-ring was done once and has reduced the current by a factor of 2.

Table 4

Damage constants and the corresponding standard deviation error for ^{60}Co-gamma irradiation .

$(I/V)/D$	(3.6±1.0)×10^{-13} Acm^{-3}rad^{-1}
$\Delta N_{eff}/D$	(2.4±0.7)×10^3 cm^{-3}rad^{-1}

V. DISCUSSION

A. *Effective Doping Concentration*

The ^{60}Co-gamma irradiations have shown that negative space charge is introduced by displacement damage even if only point defects are generated. However, since no annealing effect, especially no reverse annealing was observed it must be concluded that long term annealing effects originate from the closer spacing of the defects or the higher lattice strain present after heavy particle damage. Acceptor levels in the lower half of the band gap introduced by the gamma irradiation would be the first idea to explain the variations seen in Figure 8b). The introduction rate given in Table 4 is however around a factor 200 smaller than the introduction rates found for the dominant defect levels VO_i and C_iO_i in reference [7]. It would therefore appear to be very difficult to detect the corresponding levels after gamma irradiation. It will be noted that the corresponding factor between the introduction rates is of the order of ten for heavy particle damage. Using the Transient Current Technique (TCT) we have observed a hole trap at around E_V + 0.5 eV in both neutron and gamma irradiated samples [17]. The large hole capture cross section of around 10^{-14} cm^2 suggests that this level is an acceptor which then could account for the increase of negative space charge observed after heavily particle and ^{60}Co-gamma damage. Also the found introduction rates (0.04 cm^{-1} (n), 3000 cm^{-3}rad^{-1} (gamma)) would be in agreement with this view.

No donor removal effect similar to the observations made after neutron irradiations is observed in Figure 8b) since the data should then fall onto a straight line that intersects the N_{eff} axis at a value distinct from zero [18]. Therefore, the interaction of displacement damage defects with the initial impurity concentration remains an open question. The I-DLTS measurements performed on the unirradiated sample (Figure 7) are considered to be basic work in this respect. The method in principle allows the determination of

concentrations of the shallow doping impurities like phosphorus. Also other trap levels, *W* and *Z*, were found which are not well understood and were tentatively assigned to thermal donors, compare for example [19].

From the finding that peak *J* grows in the TSC spectra presented in Figure 6 upon excitation of state B of the bistable defect, which correlates with an increase of the full depletion voltage (i.e. the effective doping concentration in the space charge region becomes more negative) it can be concluded that the hole trap signal *J* arises from an acceptor level. Although the C_i donor level would give rise to a TSC peak at virtually the same temperature and examples of C_i complexes which break up under current injection are known in the literature (e.g. C_iP_s [20]), it is argued here that this does not apply. On the on hand, liberated C_i also exhibits an acceptor level in the upper half of the band gap (ΔH_n = 0.11 eV, σ_n = 6×10^{-15} cm^2, see [7]) that would correspond to a TSC peak around 50 K in our measurements, which is however not observed in Figure 6b). On the other hand, the level parameters found for peak *J* in the I-DLTS study (Table 3) are distinct from the data expected for the transition $C_i^{(+/0)}$ found in [7]: ΔH_p = 0.28 eV, $\sigma_p = 4\times10^{-15}$ cm^2. Especially the large capture cross section found in Table 3 would be in agreement with the assignment to an acceptor level.

Concerning the bistability of the defect it was observed in reference [16] that the dissociation of the excited state B into the two components A_1 and A_2 does not occur in the depleted region of the diode. Moreover, no transient effect was observed during the isochronous annealing study of the weakly damaged device for which $N_{eff} > 0$, i.e., in thermal equilibrium free electrons, *n,* are more abundant than holes, *p*. Only in the neutral bulk of inverted detectors, where $p > n$ as recently was confirmed by Hall-measurements [21], does the dissociation take place. Consequently, capture of free holes seems to mediate the dissociation. Moreover, this would explain why the amount of the change in ΔN_{eff} observed on the weakly damaged sample in Figure 2a) is larger compared with the more heavily damaged sample. In both cases would the bistable defect be introduced during the isochronous annealing, however, in the n-type sample state B, which introduces the negative space charge, is a stable configuration. One interesting feature of Figure 2a) is that the activation temperature for the reverse annealing processes depends on the irradiation fluence, which would qualitatively be in agreement with the modeling according to a second order reaction as outlined in [15]. Finally it is noted that the concentration of peak *J* as determined in Figure 5b) can not account for all of the change seen in N_{eff} (Figure 2a). It is however possible that the level was not filled completely and the concentration given in Figure 5b) would thus be too small. Moreover, the hole traps *Q* and N_d which were found to anneal in (Figure 4b) could turn out to be acceptors. Further TSC studies, using optical filling to characterize these new traps, are under way.

The total vacancy concentration is decreasing during elevated temperature annealing of neutron damaged high resistivity silicon, as was observed in reference [22]. The current understanding is that vacancies are liberated from the dense defect zones present after heavy particle damage. This would be in agreement with the observation made in Figure 5a) that the VO_i concentration is increasing. It would thus be expected that the peak N_b, which anneals out, is vacancy related. However, more data are needed to ascertain that N_b originates from a defect qualitatively distinct from the divacancy VV and is not just a lattice-strain induced broadening of the $VV^{(-/0)}$ transition. It has been shown in [18] that the reverse annealing effect does not depend on the initial resistivity. According to the above statements the acceptor level produced during reverse annealing should therefore arise from a higher order intrinsic point defect which might however incorporate oxygen and/or carbon, the most abundant impurities in the material (> 10^{15} cm^{-3}).

B. Leakage Current

The bulk generation leakage current anneals out continuously for temperatures ranging from 70°C to 190°C and then stays more or less constant (Figure 2b). Only one defect level in the TSC spectrum, namely, N_b, the left-hand side of peak *N*, is found to anneal out at approximately the same rate. This behavior, and also the level parameters derived for this electron trap in reference [7] (ΔH_t = 0.39 eV, $\sigma_n = 1\times10^{-15}$ cm^2), are in good agreement with the findings in [3]. It is of particular interest to note that also the maximum temperatures of the peaks *N* and *I*, which are both related to the divacancy, exhibit a jump around the 190°C annealing step (Figure 5c). Moreover, neither was leakage current annealing observed, nor does peak N_b exist in ^{60}Co-gamma irradiated devices [7]. Our results would therefore support the view of [3] that N_b is directly correlated with the large leakage currents observed after heavy particle damage. As outlined in that reference, Shockley-Read-Hall statistics is then unlikely to explain the generation processes.

Since the transition $VV^{(-/0)}$ is one of the deepest trap, it is calculated here what amount of leakage current would arise from that level. Reliable data regarding the level parameters have recently been reported by Hallén et al. [23]. Because their measurements have been performed on proton irradiated samples after 30 min annealing at 150°C the results should be applicable to the later stages of the isochronous annealing study presented here. Table 5 summarizes the level parameters calculated for a temperature of 20°C. The level position relative to the intrinsic Fermi-level E_t - E_i has been calculated according to eq. (5). To be consistent with [23] the effective masses and the band gap energy were taken from the review given in [24].

Table 5

Parameters of the $VV^{(-/0)}$ transition at 293.16 K according to reference[23].

c_n [cm^{3}s^{-1}]	c_p [cm^{3}s^{-1}]	ΔH_n [eV]	X_n	E_t-E_i [eV]	$q_0 e_n e_p/(e_n+e_p)$ [A]
5.25×10^{-8}	3.62×10^{-7}	0.421	0.33	0.113	3.97×10^{-18}

The value in the last column of Table 5 may be used in combination with eq. (7). Applying $g_t = 0.5\ cm^{-1}$ (see Figure 5a) results in $\alpha \approx 2\times10^{-18}$ A/cm which is a factor 2.5 smaller than the saturation value found in Figure 2b). Although the divacancy can account for a considerable fraction, there seem to be additional sources for the leakage current. Defects closer to the middle of the band gap would therefore be expected to exist. A deep electron trap, labeled *O*, has been observed with I-DLTS (Figure 7). It is however not clear whether this defect level was introduced by the irradiation or by the processing of the device. The previously mentioned hole trap observed in the TCT measurements [17] would appear to be a good candidate. It was however so far not possible to determine the capture coefficient for electrons which must be accurately known in order to calculate the leakage current from this trap.

VI. ACKNOWLEDGMENTS

We would like to acknowledge the members of the CERN RD48 (ROSE) collaboration for fruitful discussions. Thanks are due to J.A. Kierstead and Z. Li for supervising the ^{60}Co-gamma irradiations. Financial support is acknowledged from the BMFT under contract 05 7HH 17I.

VII. REFERENCES

[1] A. Chilingarov et al., "Radiation studies and operational projections for silicon in the ATLAS inner detector", *Nucl. Instr. and Meth. A*, 360, pp. 432-437, 1995.

[2] W. Shockley and W.T. Read, Jr., "Statistics of the recombination of holes and electrons", *Phys. Rev.*, 87, pp. 835-842, 1952.

[3] S.J. Watts et al., "A new model for generation-recombination in silicon depletion regions after neutron irradiation", presented at the IEEE Nuclear Science Radiation Effects Conference, 15-19 July 1996.

[4] G. Lutz, "Effects of deep level defects in semiconductor detectors", *Nucl. Instr. and Meth. A*, 377, pp. 234-243, 1996.

[5] S.M. Sze, "Physics of semiconductor devices, 2nd edition", John Wiley & Sons, 1981.

[6] J.A. Van Vechten and C.D. Thurmond, "Entropy of ionization and temperature variation of ionization levels of defects in semiconductors", *Phys. Rev. B*, 14, pp. 3529-3550, 1976.

[7] M. Moll et al., "Comparison of defects produced by fast neutrons and ^{60}Co-gammas in high resistivity silicon detectors using Deep Level Transient Spectroscopy", Proceedings of the International Conference on Radiation Effects on Semiconductor Materials, Detectors and Devices, Florence, Italy, 1996, to be published in NIM.

[8] J.G. Simmons and G.W. Taylor, "High-field isothermal currents and thermally stimulated currents in insulators having discrete trapping levels", *Phys. Rev. B*, 5, pp. 1619-1629, 1971.

[9] E. Borchi et al., "Leakage current, annealing, and deep defect production studies in neutron irradiated n-type Si-detectors", *Nucl. Instr. and Meth. A*, 301, pp. 215-218, 1991.

[10] V. Eremin et al., "Elevated temperature annealing of neutron induced reverse current and corresponding defect levels in low and high resistivity silicon detectors", *IEEE Trans. NS*, 42, pp. 387-393, 1995.

[11] C. Osius, diploma thesis, University of Hamburg, 1995.

[12] E. Fretwurst et al., "Development of large area silicon detectors", *Nucl. Instr. and Meth. A*, 253, pp. 467-477, 1987.

[13] R. Böttger et al., "Radiation damage studies of high resistivity silicon detectors at various neutron energies", to be published.

[14] H. Feick et al., "Analysis of TSC spectra measured on silicon pad detectors after exposure to fast neutrons", Proceedings of the International Conference on Radiation Effects on Semiconductor Materials, Detectors and Devices, Florence, Italy, 1996, to be published in NIM.

[15] E. Fretwurst et al., "Reverse annealing of the effective impurity concentration and long term operational scenario for silicon detectors in future collider experiments", *Nucl. Instr. and Meth. A*, 342, pp. 119-125, 1994.

[16] M. Moll et al., "Observation of a bistable defect generated and activated by heat treatments in irradiated high resistivity silicon detectors", *Nucl. Phys. B (Proc. Suppl.)*, 44, pp. 468-474, 1995.

[17] E. Fretwurst et al., "Investigation of damage induced defects in silicon by TCT", Proceedings of the International Conference on Radiation Effects on Semiconductor Materials, Detectors and Devices, Florence, Italy, 1996, to be published in NIM.

[18] H. Feick et al., "Long term damage studies using silicon detectors fabricated from different starting materials and irradiated with neutrons, protons, and pions", *Nucl. Instr. and Meth. A*, 377, pp. 217-223, 1996.

[19] J.L. Benton et al., "The oxygen donor effect in silicon", *Physica*, 116B, pp. 271-275, 1983.

[20] E. Gürer et al., "Configurational metastability of carbon-phosphorus pair defects in silicon", *Material Science Forum*, 83-87, pp. 339-344, 1992.

[21] U. Biggeri et al., "Self annealing effect on neutron irradiated silicon detectors by Hall effect analysis", *IEEE Trans. NS*, 43, pp. 1599-1604, 1995.

[22] Z. Li et al., "Microscopic analysis of defects in a high resistivity silicon detector irradiated to $1.7\text{x}10^{15}$ n/cm^2", *IEEE Trans. NS*, 43, pp. 1590-1598, 1996.

[23] A. Hallén et al., "Lifetime in proton irradiated silicon", *J. Appl. Phys.*, 79, pp. 3906-3914, 1996.

[24] M.A. Green, "Intrinsic concentration, effective densities of states, and effective mass in silicon", *J. Appl. Phys.*, 67, pp. 2944-2954, 1990.